Supplementary Information

$TiO(OH)_2$ can exceed the critical limit of conventional CO_2 sorbents: modification needed for high capacity and selectivity

Fan Wu [a], Paul A. Dellenback [a], Sam Toan [b], Kurt Russell [c], Maohong Fan [b, d, e, 1]

[a] Department of Mechanical Engineering, University of Wyoming, Laramie, WY 82071, USA
[b] Departments of Chemical and Petroleum Engineering, University of Wyoming, Laramie, WY 82071, USA
[c] Civil and Environmental Engineering, Stanford University, CA 94305, USA
[d] School of Energy Resources, University of Wyoming, Laramie, WY 82071, USA
[e] School of Civil and Environmental Engineering, Georgia Institute of Technology, Atlanta, GA 30332

1. Characterization of material

The pore size distribution, specific surface area, and total pore volume of the sorbents were calculated from nitrogen adsorption/desorption isotherm analysis at 77 K measured using a Quantachrome autosorb-iQ surface area and pore size analyzer, and surface area was obtained using the Brunauer–Emmet–Teller (BET) equation. The chemical structures of sorbents were characterized by Fourier transform infrared spectroscopy [(FTIR), Spectrum 100, Perkin Elemer].

As seen in Figure S1 where adsorption/desorption isotherms of $TiO(OH)_2$ at 77 K are plotted, there is an inflection point at P=0.45 Po, indicating that nitrogen adsorption has reached a point where its adsorption is kinetically hindered. The specific surface area (and pore volume) of fresh and spent $TiO(OH)_2$ (See Figure S2) is 306 and 300 m^2/g (0.435 and 0.424 cm^3/g), respectively, indicating $TiO(OH)_2$ is a stable adsorbent across 50 CO_2 adsorption/desorption cycles.

[1] Corresponding author; Email: mfan@uwyo.edu
Phone: +1 (307) 766 5633 (Maohong Fan)

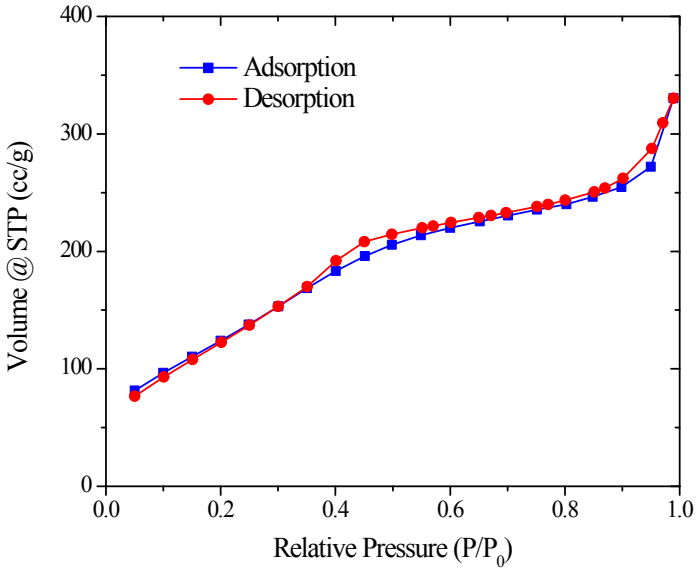

Figure S1 Nitrogen adsorption–desorption isotherms of $TiO(OH)_2$ at 77 K

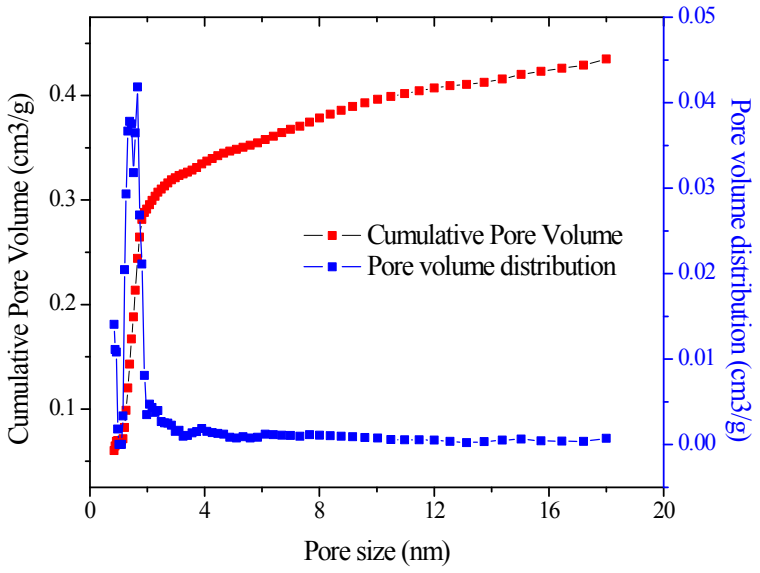

Figure S2 Pore size distribution of $TiO(OH)_2$ with DFT method (red) and total pore volume (blue) vs pore size

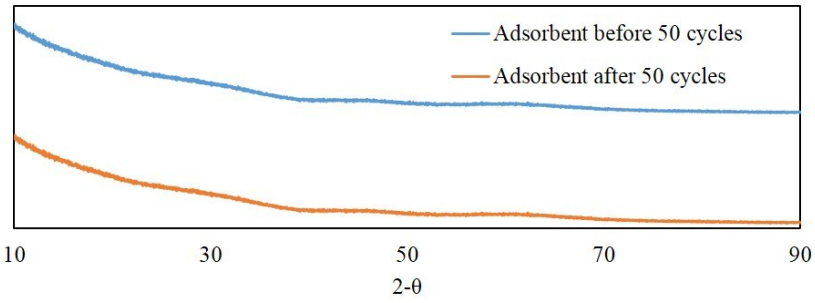

Figure S3 XRD graphs of $TiO(OH)_2$ before and after 50 cycles

XRD graphs of $TiO(OH)_2$ across 50 cycles of adsorption and desorption are shown in Figure S3.

2. CO_2/N_2 separation procedure

As seen in Figure 1, mass flow controlers (MFCs 4, 5, and 6) regulate the mole ratio of CO_2 and N_2 fed into the adsorption column (10) as either pure CO_2, pure N_2, or a mixture while back-pressure regulators maintain a stable pressure in the column. Isotherms were generated for adsorption and desorption (in that order) using dynamic measurement by using Ar as a carrier gas to feed effluent N_2 and CO_2 into the mass spectrometer (16).

The adsorption process was initiated by introducing the adsorbates (CO_2 and/or N_2) into the column through two 3-way valves, along with the Ar that was used to initially generate pressure and keep the system free from other gases. The mole flow rates of gas(es) at the inlet and outlet of the column were recorded. After adsorption was completed, Ar carrier gas was used to eliminate the adsorbed CO_2 and N_2 from the adsorption process.

The sorption capacities of the $TiO(OH)_2$ for CO_2 are calculated using (E1)[1] at different sorption pressures. The integral evaluates the total volume of the remianed gas in the system. Part of the volume is adsorbed in the material and another part fills the free volume.

$$V_{ads,CO_2} = \int_{t_0}^{t_1} (x_{0,CO_2} - x)dt \cdot \dot{V} - V_{EV} \cdot x_{0,CO_2} = V_{CO_2} - V_{EV,CO_2} \qquad \text{(E1)}$$

where, x_{0,CO_2} is the mole fraction of CO_2 in the feed gas mixture, x is the actual mole fraction of CO_2 at the outlet, $\dot{V}$ is the total input volume flow rate of the feed gas, V_{EV} is the void volume of the system (nano-pores in between particles and empty volume in tubes). The adsorbed molar amount (n_{ads}) can be evaluated from ideal gas law by using the thermodynamic conditions of the gas where the flow is measured by (E2):

$$n_{ads} = \frac{V_{CO_2} \cdot P_0}{RT} - \frac{V_{CO_2,EV} \cdot P_{EV}}{RT} \quad \text{(E2)}$$

where P_0 is the environmental pressure, P_{EV} is the pressure in the column during breakthrough, T is the temperature where the volume flow has been measured (room temperature) and R is the gas constant.

3. Langmuir-Freundlich isotherms

The Langmuir–Freundlich isotherm[2] is used to describe experimental single component adsorption equilibrium data of CO_2 and N_2, and can be described as

$$\frac{q}{q_e} = \frac{(K \cdot P)^n}{1 + (K \cdot P)^n} \quad \text{(E3)}$$

where q is the adsorption capacity of the sorbent, p is the equilibrium pressure of the adsorbate, q_e is the adsorption saturation capacity, n represents the adsorption constant on a heterogeneous surface, K is the adsorption–desorption equilibrium constant, and the parameter n is a heterogeneity factor, and the parameters are shown in Table S1.

Table S1. Langmuir–Freundlich isotherm parameters for pure CO_2 and pure N_2

	Temperature	297K	310K	323K	336K	349K
CO2	q_e (mmol/g)	21.29	15.46	10.47	10.45	10.33
	K	0.0043	0.0080	0.0107	0.0097	0.0128
	n	1.54	1.72	1.49	1.49	1.52
N2	q_e (mmol/g)	10.34	7.76	5.08	4.86	4.23
	K	0.0035	0.0006	0.0005	0.0002	0.0001
	n	1.57	1.22	1.05	1.06	1.00

The Langmuir–Freundlich adsorption isotherm model for binary adsorption systems [2] has been described by (E4) and (E5) as follows,

$$\frac{q_{N_2}}{q_{N_2,e}} = \frac{(K_{N_2} \cdot P_{N_2})^{n_{N_2}}}{1 + (K_{N_2} \cdot P_{N_2})^{n_{N_2}} + (K_{CO_2} \cdot P_{CO_2})^{n_{CO_2}}} \quad \text{(E4)}$$

$$\frac{q_{CO_2}}{q_{CO_2,e}} = \frac{(K_{CO_2} \cdot P_{CO_2})^{n_{CO_2}}}{1 + (K_{N_2} \cdot P_{N_2})^{n_{N_2}} + (K_{CO_2} \cdot P_{CO_2})^{n_{CO_2}}} \quad \text{(E5)}$$

where p_{CO2} and p_{N2}, q_{CO2} and q_{N2}, n_{CO2} and n_{N2}, and K_{CO2} and K_{N2} are the partial pressures, equilibrium adsorption capacities, adsorption constants, and adsorption–desorption equilibrium constants of CO_2 and N_2, respectively.

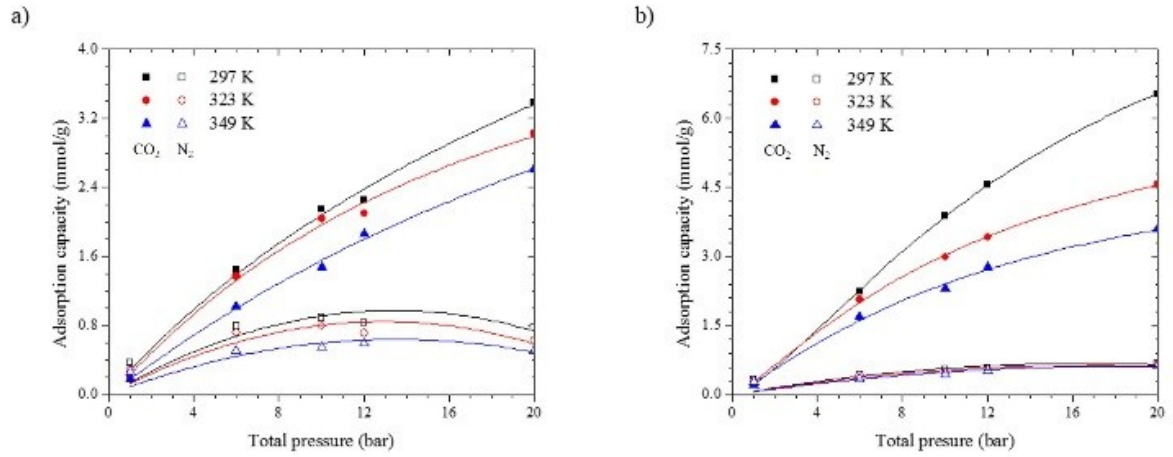

Figure S4. Adsorption equilibrium isotherm of binary CO_2/N_2 [molar ratio of (a) 25/75, (b) 75/25]

Adsorption breakthrough experiments were carried out at three different temperatures (297, 323, and 349 K) and under various feed concentrations (25/75 and 75/25 for CO_2/N_2 by volume), as shown in Figure S3.

4. Selectivity comparison

Selectivity is a method used to compare the affinity of surface for different species, and is defined as follows (E6) between species *i* and *j* [3]:

$$S_{i,j} = \frac{x_i}{y_i} / \frac{x_j}{y_j} \quad \text{(E6)}$$

where x_i and x_j are the adsorbed phase composition by volume, and y_i and y_j are the respective feed gas compositions.

Table S2 CO_2/N_2 selectivity at different feed gas CO_2/N_2 ratios

CO_2/N_2 ratio	CO_2/N_2 Selectivity		
	$TiO(OH)_2$	Activated Carbon	Zeolite

1/9	12.9	5.4	4.3
3/9	11.8	4.3	3.2
5/9	10.4	3.3	2.4
7/9	8.5	2.6	1.9
9/9	6.9	2.0	1.4
9/7	5.4	1.5	1.2
9/5	3.9	1.1	1.2
9/3	3.2	0.9	1.1
9/1	2.9	0.8	1.1

5. Sorption kinetics

The kinetic mechanism of CO_2 adsorption is also an important property when evaluating the performance of an adsorbent for CO_2 capture. In this study, pseudo-first and second-order gas solid adsorption models, which have been widely used to model and predict adsorption kinetics, were adopted to describe the adsorption kinetics and the adsorbent-adsorbate interactions. The pseudo-first order model assumes that the adsorption rate is proportional to the number of vacant adsorption sites, which can be expressed by the following equation[4,5]

$$\frac{dq_t}{dt} = K_f(q_e - q_t) \qquad \text{(E7)}$$

where q_e (mmol/g) and q_t (mmol/g) are the adsorption capacities at equilibrium and a given time, respectively, and K_f (sec^{-1}) is the first-order kinetic constant. Integration of (E7) yields

$$\ln(\frac{q_e}{q_e - q_t}) = K_f t \qquad \text{(E8)}$$

which explains surface coverage in terms of loading, q_t , and equilibrium loading, q_e, with regard to time, t.

The pseudo-second order model is based on the assumption that the adsorption rate is proportional to the square of the number of vacant adsorption sites. This model can be expressed in equation

$$\frac{dq_t}{dt} = K_s(q_e - q_t)^2 \qquad \text{(E9)}$$

where q_e (mmol/g) and q_t (mmol/g) are the adsorption capacities at equilibrium and a given time, respectively, and K_s (g/(sec•mmol)) is the second-order kinetic constant. Similar to (E7),

integration of (E9) gives:

$$\frac{1}{q_e - q_t} = K_s \, t + \frac{1}{q_e} \qquad \text{(E10)}$$

The values of K_f and K_s can be obtained by using adsorption measurements and regressing (E8) and (E10) respectively. The slope of a straight line plot from $log(1 - \frac{q_t}{q_e})^{-1}$ versus time plot of pseudo first order model gives the value of K_f. Similarly, the value of K_f can be obtained by a $1/(q_e - q_t)$ versus time plot in the pseudo second order model. Figure S4 (a) and (b) shows the comparison of the two model results and the parameters calculated are given in Table S3.

The pseudo-first order model represents the reversible interaction between the adsorbent and adsorbate, and is more inclined to predict the physical adsorption behavior on adsorbents. On the other hand, the pseudo-second order model gives better prediction on the chemical interaction between adsorbent and adsorbate caused by the strong binding of gas to the surface of adsorbent. The correlation coefficient, R^2, for pseudo-first and pseudo-second order model are 0.991 and 0.937, respectively. By comparing the values of R^2, it can be concluded that the both pseudo-first and second order model fit with the experimental data very well with pseudo-first order model giving slightly better prediction, which may imply that physical adsorption may play a stronger role to the high adsorption-desorption rates.

Table S3. Pseudo first and second order rate constants

Pseudu-first order			Pseudo-second order		
K_f (sec^{-1})	Rate equation	R^2	K_s (g/(mmol•sec))	Rate equation	R^2
0.0013	$ln(\frac{q_e}{q_e - q_t}) = K_f t$	0.991	0.2083	$\frac{1}{q_e - q_t} = K_f t + \frac{1}{q_e}$	0.937

a) b)

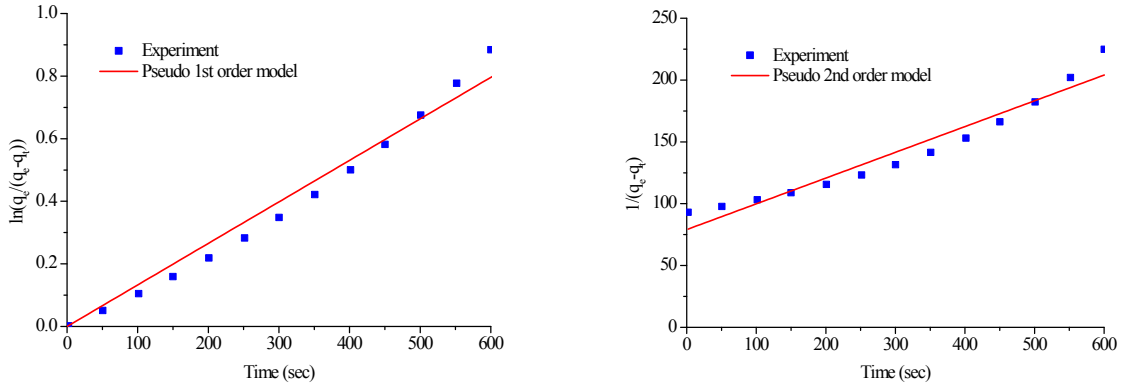

Figure S5 Pseudo 1st (left) and 2nd (right) order adsorption model

References

1 S. García, M. V. Gil, C. F. Martín, J. J. Pis, F. Rubiera and C. Pevida, *Chem. Eng. J.*, 2011, **171**, 549–556.

2 R. T. Yang, *Adsorbents: Fundamentals and Applications*, John Wiley & Sons, Ner Jersey, 2003.

3 R. T. Yang, *Gas saparation by adsorption processes*, Imperial College Press, London, 1997.

4 C. Goel, H. Bhunia and P. K. Bajpai, *J. Environ. Chem. Eng.*, 2016, **4**, 346–356.

5 S. Hafeez, X. Fan, A. Hussain and C. F. Martín, *J. Environ. Sci. (China)*, 2015, **35**, 163–71.